A Dynamic Simulation Model of Outdoor Swimming Pool with Thermal Energy Storage, Boiler and Solar Thermal Collectors

Pierre Clément Blaud[1] Imad Mourtaji[1]

[1]Akkodis Research, Akkodis, France, {firstname.surname}@akkodis.com

Abstract

Outdoor swimming pool facilities are significant energy consumers, primarily due to the need to maintain thermal comfort for swimmers, as the pool is exposed to wind and outdoor air. To address the challenge of reducing energy consumption, effective simulation of the dynamical system is essential to identify energy-saving solutions. This paper presents a comprehensive implementation of an outdoor swimming pool simulation model using the Modelica programming language. The simulation model also incorporates a thermal storage system, a boiler, and a solar thermal collector, allowing a detailed analysis of the system. In addition, an in-depth explanation of the physical equations governing the swimming pool is provided, along with the methodology used to construct the Modelica model. The results show that the model allows the simulation of the thermal behavior of an outdoor swimming pool, including various heat losses, solar heat gains, and heat production from the boiler and solar collectors.

Keywords: Swimming pool model, energy system, thermal storage, boiler, solar thermal collectors

1 Introduction

In late 2017, France had 4,135 public swimming pool facilities comprising 6,412 pools and covering a total area of 1.6 million square meters (Cour des comptes 2018). These facilities represent a significant financial burden for local communities, both due to the need to offer affordable access to the public and the high levels of energy consumption required for operation (Delgado Marín, Vera García, and García Cascales 2019). A large proportion of these facilities are aging, with more than 70% built before 1995 (Cour des comptes 2018). The recent energy crisis has further exacerbated the situation, leading to increased operational costs and in some cases, full or partial closures during the winter months (Cour des comptes 2018; Delgado Marín, Vera García, and García Cascales 2019). The high energy consumption associated with these facilities arises from the need to heat large volumes of water to maintaining temperatures between 25°C and 28°C as recommended by the World Aquatics Federation, as well as to power auxiliary systems such as showers, ventilation, lighting, and administrative areas. Modeling the dynamic behavior of public swimming pools and their associated energy systems is essential for analyzing energy use and developing advanced control strategies for heating systems (Li et al. 2021).

Numerous studies have focused on the modeling of indoor swimming pools (Yuan et al. 2021; Kühn et al. 2022), outdoor swimming pools (Buscemi et al. 2024; Bernhard et al. 2019), and the integration of swimming pools with heat production systems (Li et al. 2021). Several of these works use multi-domain modeling languages such as TRNSYS (Delgado Marín, Vera García, and García Cascales 2019; Starke et al. 2017; Liu, Kim, and Shin 2021) or Modelica (Kühn et al. 2022). In the study (Delgado Marín, Vera García, and García Cascales 2019), TRNSYS was used as a simulation platform for implementing predictive control strategies. Their results demonstrated that predictive control significantly reduces energy consumption compared to traditional proportional-integral-derivative (PID) controllers. In the study (Starke et al. 2017) conducted a technical and economic analysis of a pool equipped with solar thermal heating and a heat pump, concluding that this configuration improves energy efficiency. Similarly in (Liu, Kim, and Shin 2021), the authors used TRNSYS to model a swimming pool and adjacent buildings, examining the feasibility of using a fuel cell cogeneration unit for heat and power generation. Although the system was found to be economically viable, the payback period exceeded 10 years. It can be observed that detailed modeling of swimming pool systems with TRNSYS simulation tool is well established in the literature. However, concerning the Modelica modeling language, few studies have addressed swimming pool systems coupled with heat sources, to our knowledge, only one of these studies focused on an indoor swimming pool (Kühn et al. 2022), without considering an outdoor pool and several heat sources.

In the present work, we model a public outdoor swimming pool using the Modelica language including an external pool, consequences of weather conditions on the pool, a thermal energy storage unit and two heat sources: a boiler and a solar thermal collector. The main contributions of this work are:

- The implementation and simulation of a public outdoor swimming pool with consideration of external environment and thermal cover modeling using the Modelica language;
- The development of a complete energy system sim-

ulation that includes thermal energy storage (TES), and two heat sources, with a boiler, and a solar thermal collector (STC);

- And finally to propose a realistic comparative analysis of heat losses, and energy savings with and without the use of solar thermal collectors.

This paper is organized as follows: Section 2 introduces the simulation models; Section 3 depicts experimental setup; Section 4 presents the results of the work; and Section 5 concludes the work.

2 Simulation Model

2.1 Swimming Pool Model

The complete model of the swimming pool is shown in Figure 1. In the following sections, each submodel will be presented in detail.

2.1.1 Energy balance

Figure 2 depicts the energy balance without thermal cover. Assuming that the pool water is fully mixed, the temperature dynamics are governed by the following energy balance equation (Gauthier-Clerc et al. 2023; Buscemi et al. 2024) :

$$V_p \rho_w c_{p,w} \frac{dT_p}{dt} = \dot{Q}_{tot} \quad (1)$$

$$\dot{Q}_{tot} = \dot{Q}_{sun} + \dot{Q}_{heat} - \dot{Q}_{conv} - \dot{Q}_{evap} - \dot{Q}_{rad} - \dot{Q}_{cond} - \dot{Q}_{re} \quad (2)$$

with V_p the volume of the pool, ρ_w the density of water, $c_{p,w}$ the specific heat of water, $\dot{Q}_{sun}$ the heat gain from solar irradiance, $\dot{Q}_{heat}$ the heat power from the heating, $\dot{Q}_{conv}$ the heat loss from convection, $\dot{Q}_{evap}$ the heat loss from the evaporation, $\dot{Q}_{rad}$ the heat loss from the radiation, $\dot{Q}_{cond}$ the heat loss from conduction and $\dot{Q}_{re}$ the heat loss from water refilling and recycling. For the rest of the work, conduction losses are neglected as it contributes to less than 1% of total energy losses (Buscemi et al. 2024).

During the night, it is preferable to cover the pool to reduce heat loss, in this case the energy balance is depicted in Figure 3. The temperature dynamic is equal to (Buscemi et al. 2024):

$$V_p \rho_w c_{p,w} \frac{dT_p}{dt} = \dot{Q}_{heat} + \dot{Q}_{cover} - (\dot{Q}_{cond} + \dot{Q}_{re}) \quad (3)$$

$$\dot{Q}_c \simeq \dot{Q}_{sun} - (\dot{Q}_{conv} + \dot{Q}_{rad}) \quad (4)$$

with V_p the volume of the pool, ρ_w the density of water, $c_{p,w}$ the specific heat of water, T_p the pool water temperature, $\dot{Q}_{sun}$ the heat power from the solar irradiance, $\dot{Q}_{heat}$ the heat power from the heating, $\dot{Q}_{conv}$ the heat loss from convection, $\dot{Q}_{evap}$ the heat loss from the evaporation, $\dot{Q}_{rad}$ the heat loss from the radiation, $\dot{Q}_{cond}$ the heat loss from conduction, $\dot{Q}_{re}$ the heat loss from water refilling and recycling, and with $\dot{Q}_c$ the heat exchange from the pool to the cover.

2.1.2 Solar gain

Since solar irradiance can heat the pool water, the governing equation is equal to (Buscemi et al. 2024):

$$\dot{Q}_{sun} = G_h \alpha_p A_p \quad (5)$$

with G_h the global horizontal solar irradiance, α_p the solar absorptance of the pool and A_p the pool area. The solar absorptance of the pool depends on whether the pool is covered or not by the thermal cover. When the pool is not covered, the absorptance of the pool is equivalent to the absorptance of water (Buscemi et al. 2024). The Modelica graphical implementation is provided in Figure 4. An ideal prescribed heating power is implemented, and a switch controls the flow of covered or uncovered water. Both pool area and solar absorptance gains are incorporated.

2.1.3 Evaporation losses

Evaporation produces a transfer of mass and heat and occurs on the surface of a saturated liquid. This process is enhanced by both natural and forced convection, the latter being induced by wind in the case of outdoor pools (Buscemi et al. 2024). The heat losses due to evaporation are described as (Buscemi et al. 2024):

$$\dot{Q}_{evap} = \dot{E}_p \Delta H_w A_p \quad (6)$$

with $\dot{Q}_{evap}$ the heat loss from the evaporation, $\dot{E}_p$ the rate of evaporation of water, ΔH_w the latent heat of vaporization of water, A_p the pool area. When the thermal cover is unfolded, the evaporation does not occur, $\dot{Q}_{evap} = 0$. The rate of evaporation of water with forced convection and natural convection is equal to (Buscemi et al. 2024):

$$\dot{E}_{p,fc} = (0.28 + 0.784 v_{wi}) \frac{(p_{v,i} - p_{v,e})^{0.695}}{\Delta H_w} \quad (7)$$

$$\dot{E}_{p,nc} = h_m (\rho_{v,i} - \rho_{v,e}) \quad (8)$$

with $\dot{E}_{p,fc}$ the forced convection rate of evaporation, v_{wi} the wind velocity, $p_{v,i}$ the vapor pressure at the water surface depends to the saturated vapor pressure at pool temperature, $p_{v,i} = p_{vs}(T_p)$, $p_{v,e}$ the vapor pressure of the free stream depends to the saturated vapor pressure at air temperature $p_{v,e} = p_{vs}(T_a)(\frac{RH_e}{100})$, ΔH_w the latent heat of vaporization of water, $\dot{E}_{p,nc}$ the natural convection rate of evaporation, h_m the transfer coefficient for natural convection, $\rho_{v,i}$ the vapor density at the water surface and $\rho_{v,e}$ the free stream vapor density. The total rate of evaporation of the pool with the natural and forced convection is (Buscemi et al. 2024):

$$\dot{E}_p = F_A \left(\dot{E}_{p,nc}^{7/2} + \dot{E}_{p,fc}^{7/2} \right)^{2/7} \quad (9)$$

with $\dot{E}_p$ the pool rate of evaporation, $\dot{E}_{p,nc}$ the natural convection rate of evaporation, $\dot{E}_{p,fc}$ the forced convection rate of evaporation and F_A the evaporation surface

DOI 10.3384/ecp218891

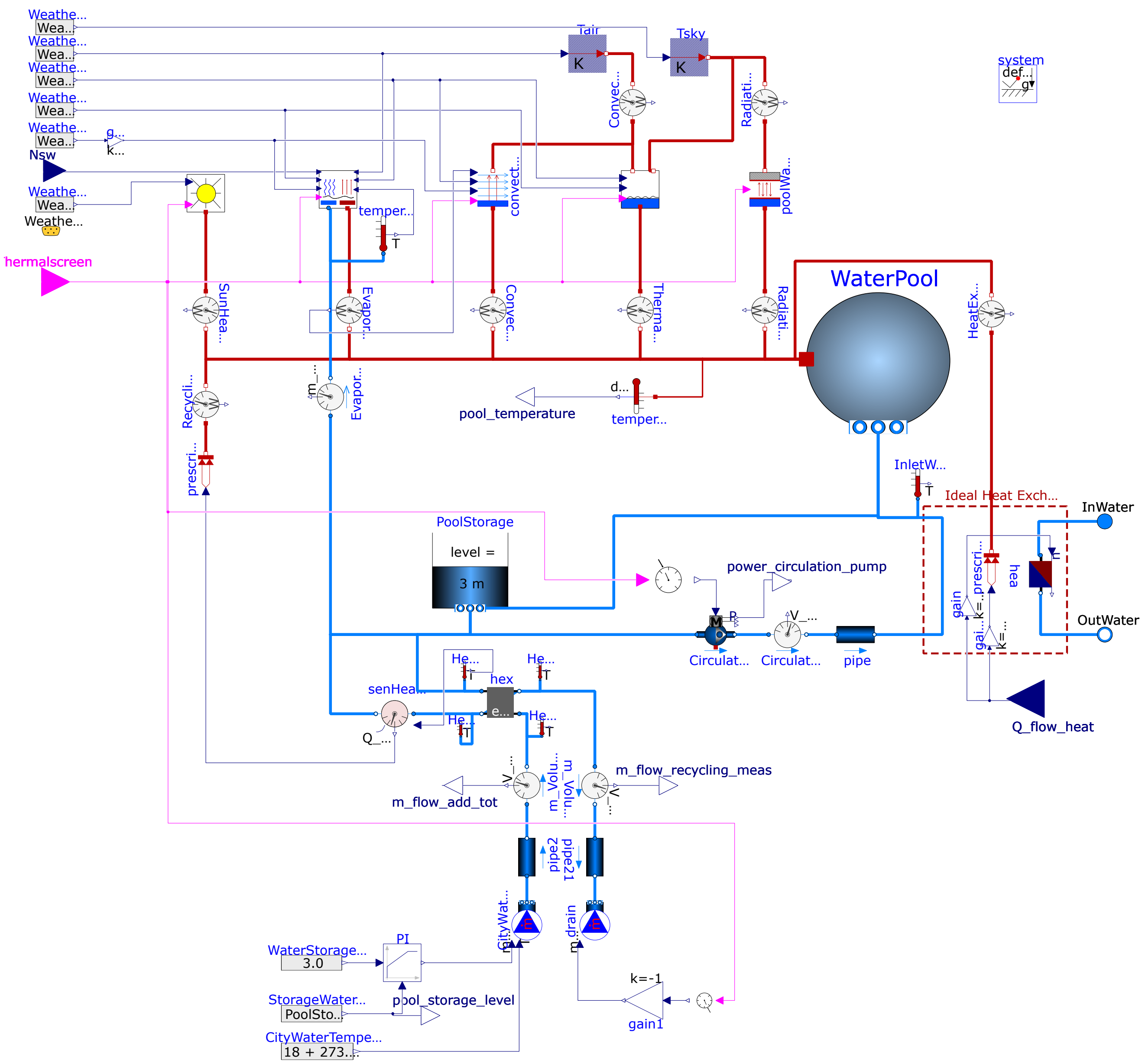

Figure 1. Model of the outdoor swimming pool.

enhancement which depends on the number of swimmer. The evaporation surface enhancement factor F_A is equal to (Buscemi et al. 2024):

$$F_A(F_u) = 1 + 2.3F_u \text{ if } F_u < 0.1 \tag{10}$$

$$F_A(F_u) = 1.2 + 0.3F_u \text{ if } 0.1 \leq F_u \leq 1 \tag{11}$$

$$F_A(F_u) = 1.5 \text{ if } F_u > 1 \tag{12}$$

with F_u the utilization factor of the outdoor swimming pool. The utilization factor is equal to (Buscemi et al. 2024):

$$F_u = \frac{A_{max}}{A_p} N_{sw} \tag{13}$$

with A_{max} the pool area per swimming pool when maximum occupancy, A_p the pool area and N_{sw} the number of swimmers inside the pool.

To calculate the transfer of mass and heat from the evaporation losses within the program, two controlled sources are implemented, one for the transfer of water and the second for heat transfer Figure 5. In addition, a program is written to control the controllable sources Listing 1. A numerical difficulty arises from the calculation of density and pressure differences, Equation 7 is no longer valid. A conditional evaluation was added and set to $\dot{E}_{p,nc}$ or $\dot{E}_{p,fc}$ when both differences become negative.

Listing 1. Sub-model program view of the modeling of the evaporation loss (heat and water loss).

```
...
equation
  Tf = (WaterTemperature + Tair)/2;
```

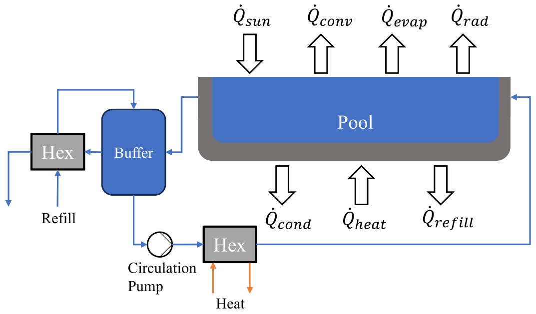

Figure 2. Energy balance of pool without thermal cover.

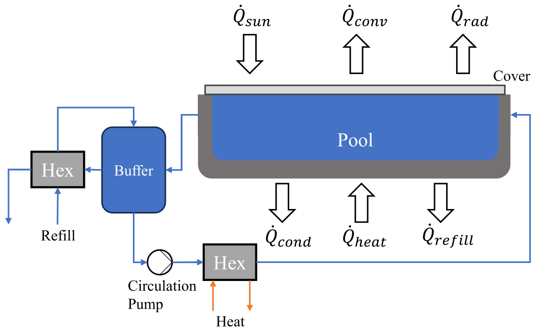

Figure 3. Energy balance of pool with thermal cover.

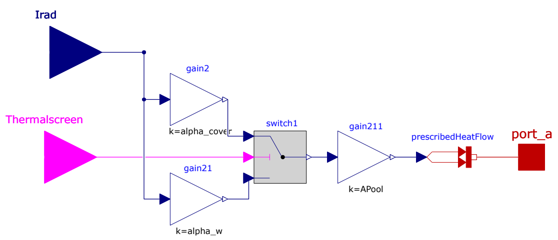

Figure 4. Sub-model of the modeling of the solar gain for the outdoor swimming pool.

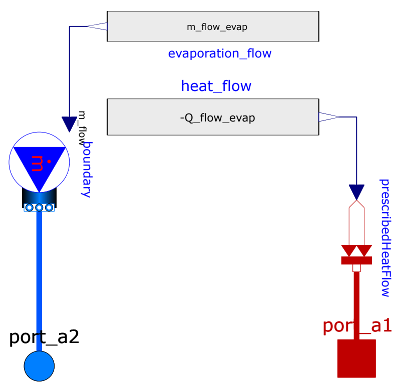

Figure 5. Sub-model graphical view of the modeling of the evaporation loss (for simplification only the equation part is presented).

```
pvi = psat_TPool;
pve = psat_TAir*(RHair/100);

if ThermalScreen == true then
    Eunfc = 0.0;
    Eunnc = 0.0;
    Eun = 0.0;
    hm = 0.0;
    Ral = 0.0;
    Sh = 0.0;
    Fu = 0.0;
    Fa = 0.0;
    Dwaf = 0.0;
    m_flow_evap = 0.0;
    Q_flow_evap = 0.0;
    delta_rho=0.0;
    delta_p=0.0;
else
    Fu = (Amax/Ap)*Nsw;
    if Fu < 0.1 then
      Fa = 1 + 2.3*Fu;
    elseif (0.1 <= Fu) and (Fu < 1) then
      Fa = 1.2 + 0.3*Fu;
    else
      Fa = 1.5;
    end if;
    Dwaf = (1.049*10^(-4)/pAtm)*Tf^1.774;
    Ral = (g_n*abs(rho_vi - rho_ve)*Lch^3)
        /(mudaf*Dwaf);
    if Ral < 10^7 then
      Sh = 0.54*Ral^(1/4);
    else
      Sh = 0.15*Ral^(1/3);
    end if;
    hm = Sh*Dwaf/Lch;

    delta_rho = (rho_vi - rho_ve);
    delta_p = (pvi - pve);
    if (delta_rho > 1e-4) and (delta_p > 1)
          then
        Eunnc = hm*(rho_vi - rho_ve);
        Eunfc = (0.28 + 0.784*vwind)*(((pvi
            - pve)^(0.695))/ hVap);
        Eun = (Eunfc^(7/2)+Eunnc^(7/2))
            ^(2/7);
    elseif (delta_rho <= 1e-4) and (delta_p
         > 1) then
       Eunnc = 0.0;
       Eunfc = (0.28 + 0.784*vwind)*(((pvi
           - pve)^(0.695))/ hVap);
       Eun = Eunfc;
    elseif (delta_rho > 1e-4) and (delta_p
        <= 1) then
        Eunnc = hm*(rho_vi - rho_ve);
        Eunfc = 0.0;
        Eun = Eunnc;
    else
        Eunnc = 0.0;
        Eunfc = 0.0;
        Eun = 0.0;
    end if;

    m_flow_evap = -(Fa*Eun*Ap);
    Q_flow_evap = Fa*Eun*Ap*hVap;
end if;
...
```

2.1.4 Convective losses

Convective losses are computed based on the Bowen approach (Buscemi et al. 2024):

$$\dot{Q}_{conv} = R_{Bo}\dot{Q}_{eva} \quad (14)$$

with $\dot{Q}_{conv}$ the heat loss from convection, R_{Bo} the Bowen ratio, and $\dot{Q}_{eva}$ the heat loss from evaporation. The Bowen ratio is equal to (Buscemi et al. 2024):

$$R_{Bo} = \left(\frac{c_{pa,e}p_{a,tot}}{0.622\Delta H_w}\right)\left(\frac{T_p - T_a}{p_{v,i} - p_{v,e}}\right) \quad (15)$$

with R_{Bo} the Bowen ratio, $c_{pa,e}$ the specific heat of air, p_a the air pressure, ΔH_w the latent heat of vaporization of water, T_p the pool water temperature, T_a the air temperature, $p_{v,i}$ the vapor pressure at the water surface and $p_{v,e}$ the vapor pressure of the free stream.

The implementation of convective losses is visible in the list 2. It includes an if-else condition regarding the thermal cover unfolded according to Equation 14 and Equation 15. In addition, there is a numerical issue regarding the Bowen ratio implementation, if vapor pressure at the water surface is equivalent to vapor pressure of the free stream, Equation 15 is no longer valid (division by zero). Especially since, according to (Woolley, Harrington, and Modera 2011), the Bowen ratio could have negative values and convection contributes to heat water. When the Bowen ratio approaches zero, the convective loss is zero (Woolley, Harrington, and Modera 2011), as such, the numerical implements a conditional evaluation with hysteresis with 500 Pascal and 600 Pascal for low and high threshold respectively, and is set to zero.

Listing 2. Sub-model program view of the modeling of the convective losses.

```
...
equation
  Tair = fluid.T;
  Twater = solid.T;
  pvi = psat_TPool;
  pve = psat_TAir*(RH/100);

  if thermalScreen == false then
    Q_flow = Rbo*Qevap;
    delta_p = (pvi - pve);
    if hysteresis.y == true then
      Rbo = (cp_TAir*pAtm/(0.622*hVap))*((
          solid.T - fluid.T)/(pvi - pve));
    else
      Rbo = 0.0;
    end if;
  else
    Q_flow = 0;
    Rbo = 0;
    delta_p = 0;
  end if;
  solid.Q_flow = Q_flow;
  fluid.Q_flow = -Q_flow;
...
```

2.1.5 Radiative losses

The Stefan-Boltzmann equation is used in this work to calculate the radiative heat flow losses between the water surface and the environment (Buscemi et al. 2024):

$$\dot{Q}_{rad} = \sigma\varepsilon_p A_p(T_p^4 - T_{sky}^4) \quad (16)$$

with σ the Stefan-Boltzmann constant, ε_p the long wave emissivity of the pool, A_p the pool surface area, T_p the pool water temperature and T_{sky} the sky temperature. The sky view factor is not considered as it is considered equal to one (Buscemi et al. 2024).

The implementation of the radiative heat flow is visible in Listing 3. It includes an if-else rule regarding the thermal cover unfols.

Listing 3. Sub-model program view of the modeling of the radiative losses.

```
...
equation
  if thermalScreen == false then
    Q_flow = epsilon_p*APool*Modelica.
        Constants.sigma*(port_a.T^4 -
        port_b.T^4);
  else
    Q_flow = 0.0;
  end if;
...
```

2.1.6 Thermal cover losses

When the thermal cover is unfolded, it is in direct contact with the pool water, the heat from the pool is released by conduction on the cover material then by convection and by radiation from the cover to the outside environment. The conduction heat flow of the thermal cover is equal to (Buscemi et al. 2024):

$$\dot{Q}_c = \frac{\lambda_c}{s_c}(T_c - T_p)A_p \quad (17)$$

with $\dot{Q}_c$ the heat flow of the thermal cover, λ_c the thermal conductivity of the cover, s_c the thickness of the cover, T_c the cover temperature and A_p the pool surface area. The convective heat loss of the thermal cover is defined as (Buscemi et al. 2024):

$$\dot{Q}_{conv} = h_{conv}A_p(T_c - T_a) \quad (18)$$

with $\dot{Q}_{conv}$ the convective heat flow of the thermal cover, h_{conv} the variable convective coefficient, T_c the cover temperature and T_a the air temperature. The radiative heat flow losses between the cover surface and the environment is equal to (Buscemi et al. 2024):

$$\dot{Q}_{rad} = \sigma\varepsilon_c A_p(T_c^4 - T_{sky}^4) \quad (19)$$

with σ the Stefan-Boltzmann equation, ε_c the long wave emissivity of the cover, A_p the pool surface area, T_c the cover temperature and T_{sky} the sky temperature.

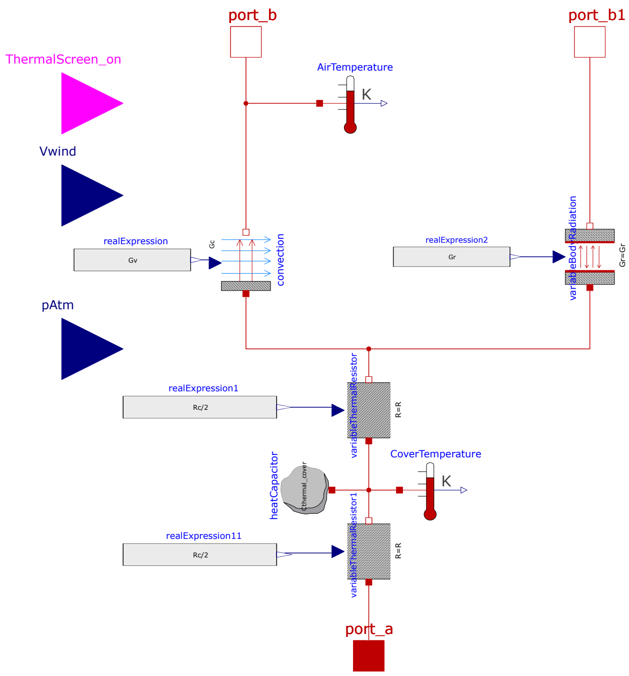

Figure 6. Modeling of the heat flow of the thermal cover.

Thermal cover model model consists of a graphical component, as shown in Figure 6, along with a text-based program designed to calculate the varying thermal coefficients, as detailed in Listing 4.

Listing 4. Sub-model program view of the modeling of the thermal cover heat flow.

```
...
equation
  Tf = (Tthermal_screen + Tair)/2;
  if ThermalScreen_on == true then
    Rc = Rts;
    Gr = epsilon_c*APool;
    Ral = (g_n*abs(Tthermal_screen - Tair)
        *(Lch^3)*Pr)/(Tf*eta_air_Tf^2);
    if Tthermal_screen > Tair then
      if Ral < 10^7 then
        Nul = 0.54*Ral^(1/4);
      else
        Nul = 0.15*Ral^(1/3);
      end if;
    else
      Nul = 0.52*Ral^(1/5);
    end if;
    hnc = ((lambda_air_Tf*Nul)/Lch);
    hfc = (5.7*Vwind^(0.8)*Lch^(-0.2));
    Gv = (hnc^(7/2) + hfc^(7/2))^(2/7) *
        APool;
  else
    Ral = 0.0;
    Nul = 0.0;
    hnc = 0.0;
    hfc = 0.0;
    Gr = 0.0;
    Rc = Rts;
    Gv = 0.0;
  end if;
...
```

2.1.7 Heating power

The heat source Q_{heat} for outdoor swimming pools incorporates a water-to-water heat exchanger (Buscemi et al. 2024). An ideal heat exchanger is utilized within the Modelica model, featuring an external circuit connected to the swimming pool to draw energy from the network. This system is coupled with an ideal heat source to supply heat to the water pool model, as illustrated in Figure 1.

2.1.8 Water buffer and recycling

The pool includes a water buffer volume designed to store excess water when swimmers are present, as well as to facilitate the addition of fresh water (Gauthier-Clerc et al. 2023). This fresh water is introduced through a heat exchanger that exchanges heat with gray water. Within Modelica implementation, a controlled water source removes gray water, while a second water source, controlled by a PI controller, maintains a constant water level in the buffer volume. When water volume decreases due to evaporation or removal, the controlled water source adds fresh water Figure 1.

2.2 Energy Systems Model

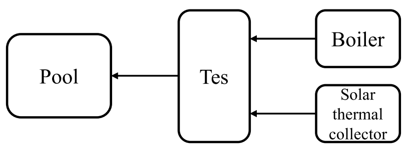

Figure 7. Block diagram of the considered energy system, constituted of pool, TES, boiler and STC.

The block diagram in Figure 7 illustrates the energy system used in the simulation. The swimming pool is modeled as a heat-consuming unit, while TES unit can either store or release heat to the pool. Two heat sources are integrated into the system: a boiler and an STC. The heat generated by the boiler can be directly controlled, whereas the heat produced by the STC depends on solar radiation and cannot be controlled actively. All three components originate from the AixLib Modelica library (Maier et al. 2024), and they are interconnected via pumps and fluid interfaces, as shown in Figure 8. The pool temperature is regulated using a proportional integral controller, while the boiler is managed by a hysteresis control system: the boiler operates at full capacity when the TES temperature falls below a defined minimum, and it turns off when the temperature reaches a specified upper limit. The STC is not actively controlled; instead, its heat output is directly delivered to the TES.

3 Experimental Setup

The swimming pool and associated energy systems were modeled using OpenModelica (Fritzson 2011) version

DOI
10.3384/ecp218891

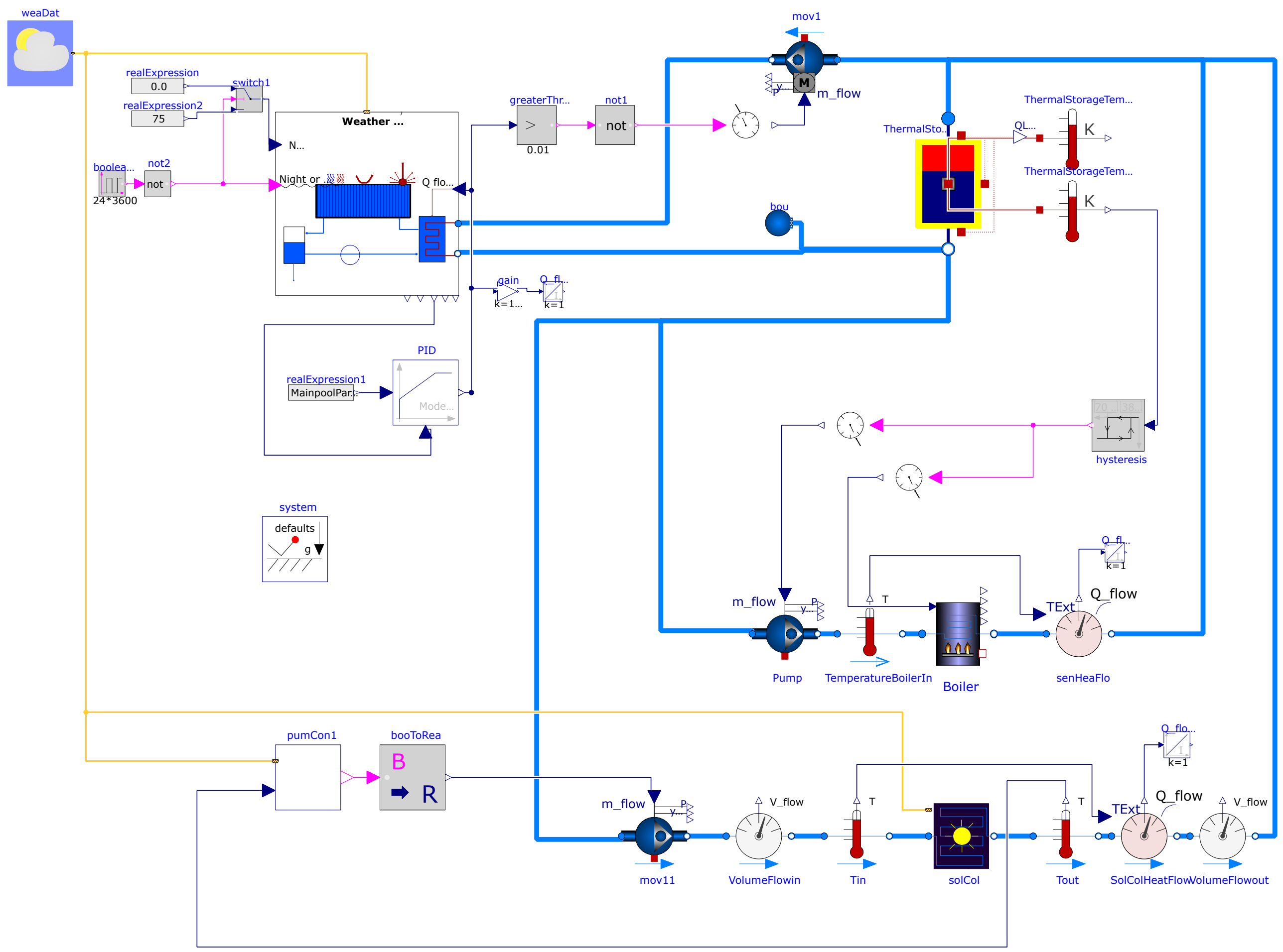

Figure 8. Model of the modeling of the energy system considering the swimming pool, the TES, the boiler and the STC.

1.23.1. Simulations were executed using the Dassl solver (Petzold 1982) on a laptop running Windows, equipped with an AMD Ryzen 7 PRO 7730U CPU and 32 GB of RAM. The system parameters are summarized as follows: Swimming pool: Table 1; Boiler, TES and STC: Table 2. Weather data were synthesized using Typical Meteorological Year (TMY) files for the city of Montpellier, France (*Repository of Building Simulation Climate Data* 2025). These data enabled integration of the AixLib meteorological model (Maier et al. 2024). To adapt the wind speed from the weather station to the pool surface and Equation 7, a 0.35 coefficient wind adjustment was used. One simulation scenario was performed, in which the pool water temperature was regulated at $28°C$. The boiler operation was managed by a hysteresis controller applied to the TES: the boiler was activated when the TES temperature dropped below the lower threshold and deactivated when the temperature exceeded the upper threshold.

4 Results

Figure 9 presents the simulation results, including the thermal power delivered by the heat exchanger, as well as the air, sky, and pool water temperatures. The pool water temperature is successfully maintained at $28°C$ throughout the simulation period. Air temperature ranges from a minimum of $5°C$ to a maximum of $39°C$, while sky temperature varies from $-12.5°C$ to $37.5°C$. The PI controller regulates the heating power between 0 and $5,000kW$ to maintain the target water temperature. Notably, between $4,000h$ and $6,000h$, the heating demand exceeds $2,000kW$, despite elevated air and sky temperatures approaching $28°C$. A reduction in heating demand was expected during this summer period, yet evaporation losses contribute significantly to increased thermal requirements.

Figure 10 shows the evolution of the different thermal losses: radiative (Figure 10.a), thermal cover (Figure 10.b), convective (Figure 10.c), evaporative (Figure 10.d) and fresh water heating (Figure 10.c). Radiative losses range from $0kW$ to $250kW$ and are more pronounced during winter ($0h$-$2,000h$ and $6,000h$-end), exceeding $150kW$. During summer ($4,000h$ –$6,000h$), they remain below $100kW$, Figure 10.a. Thermal cover losses (Figure 10.b) range from $0kW$ to $400kW$, with noticeable reductions during summer due to more favorable ambient conditions. Convective losses can be either positive

Table 1. Outdoor swimming pool parameters.

Parameters	*Descriptions*	*Value*	*Unit*	*References*
V_p	Volume	3,750	m^3	(World Aquatics 2024)
A_p	Area	1,250	m^2	(World Aquatics 2024)
L_{ch_p}	Parametric length	8.33	m	(World Aquatics 2024)
D_p	Depth	3.0	m	(World Aquatics 2024)
V_{sto}	Buffer volume	30.0	m^3	(Gauthier-Clerc et al. 2023)
T_p	Reference temperature	28.0	$°C$	(World Aquatics 2021)
$\dot{V}_{flow}$	Circulation flow	250	m^3/h	(World Aquatics 2021)
$\dot{V}_{recy}$	Recycling flow	$5\%V_p$	m^3/day	(Delgado Marín, Vera García, and García Cascales 2019)
ε_c	Cover emissivity	0.5	$-$	(Li et al. 2021)
ε_w	Water emissivity	0.95	$-$	(Buscemi et al. 2024)
α_c	Cover absorptance	0.65	$-$	Author's estimate from grey material
α_w	Water absorptance	0.85	$-$	(Buscemi et al. 2024)
λ_c	Cover conductivity	0.65	$W/(m^2K)$	(Li et al. 2021)
N_{sw}	Number of swimmers	75	$-$	Author's estimate
-	Opening hour	12	$hours/day$	Author's estimate

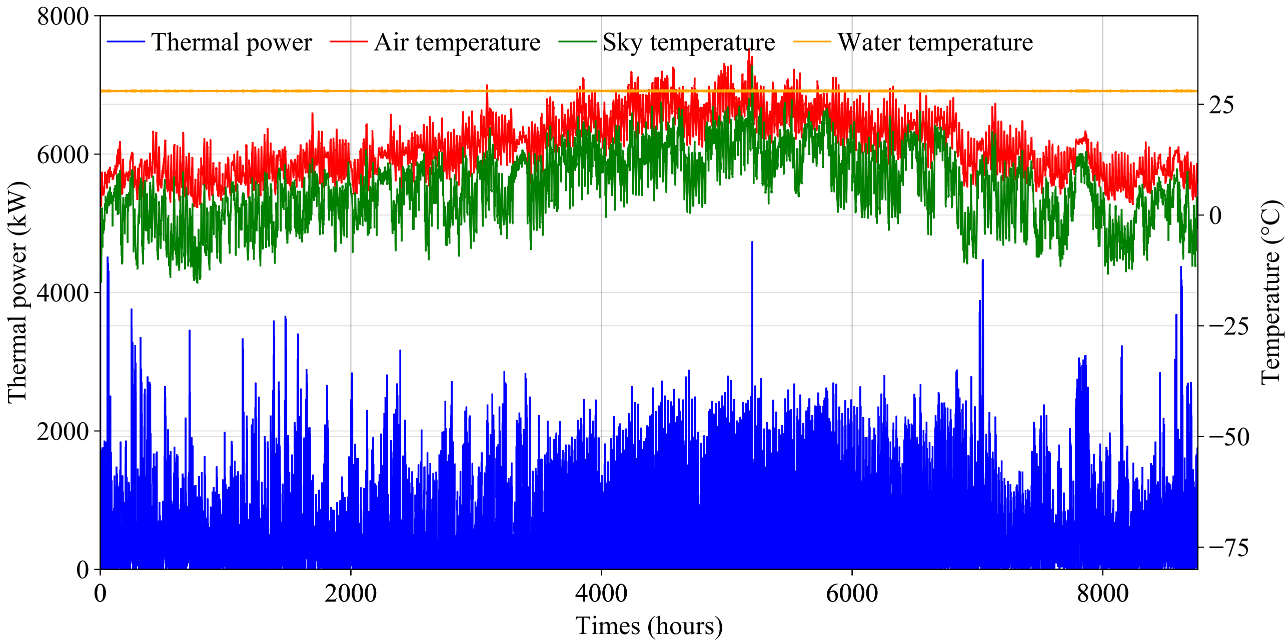

Figure 9. Temporal variation of heat exchanger thermal power, air temperature, sky temperature and pool water temperature.

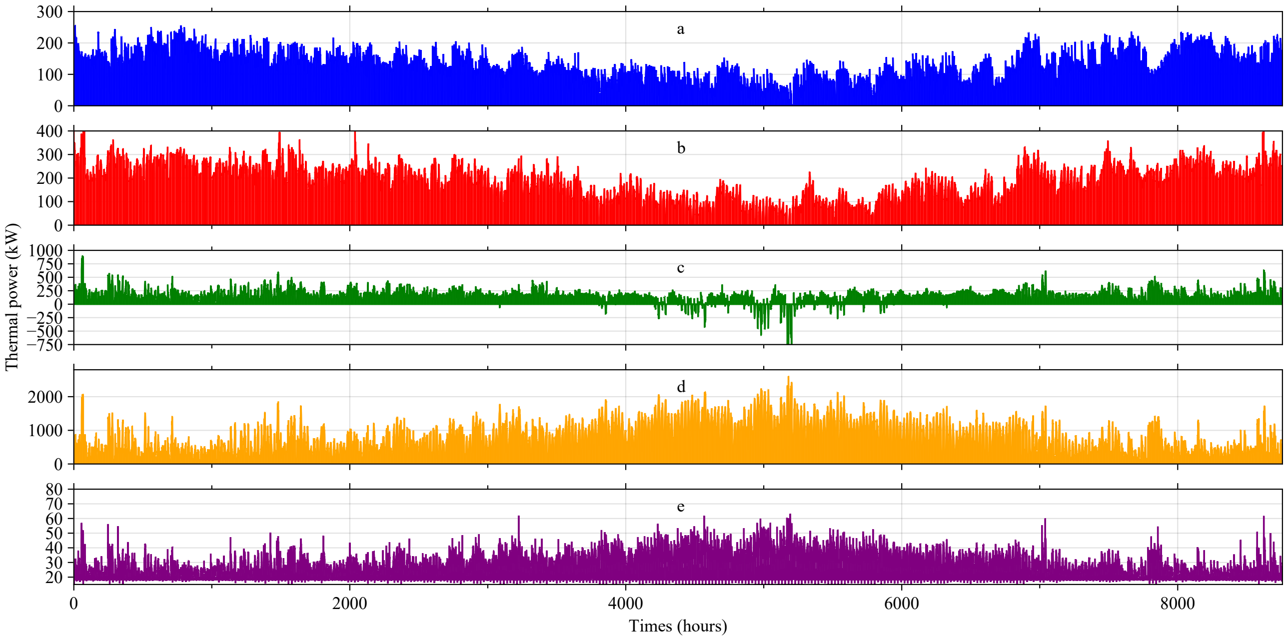

Figure 10. Temporal variation of pool thermal losses. (a) Depicts the radiative losses. (b) Depicts the thermal cover losses. (c) Depicts the convective losses. (d) Depicts the evaporation losses. (e) Depicts the fresh water losses.

Table 2. Boiler, TES and STC parameters.

System	*Parameter*	*Value*	*Unit*
Boiler	Nominal power	6	*MW*
Boiler	Minimum load	30	%
Boiler	Maximum load	100	%
Boiler	Low threshold hysteresis	40	$°C$
Boiler	High threshold hysteresis	70	$°C$
TES	Volume	800	m^3
STC	Azimuth angle	30	°
STC	Tilt angle	−180	°
STC	Ground reflectance	20	%
STC	Total area	900	m^2
STC	Collector system	Tube	-

or negative, depending on the Bowen ratio. Notable, at $4,500h$, $5,000h$ and $5,100h$, the pool gains heat from the surrounding air through convection, with power values reaching up to $750kW$. In other periods, convective heat losses reach peaks of up to $875kW$. Evaporative losses (Figure 10.d) are null when the thermal cover is in place but can reach up to $2,500kW$ during uncovered periods, especially in the summer. These losses largely explain the increase in heating demand observed from $4,000h$ to $6,000h$. Fresh water heat losses (Figure 10.e) range from 20 to $60kW$, with lower values observed at night when the pool is covered. These losses correspond to the energy required to heat the replacement water that compensates for evaporation.

Figure 11 illustrates the overall distribution of thermal losses and heat sources. Evaporation accounts for the largest share of thermal losses (63.3%), followed by thermal cover (12.97%), convection (11.33%), radiation (8.88%) and fresh water heating (3.5%). Regarding heat inputs (Figure 11.b), solar heat contributes 25.14% of the total, while the remaining 74.85% is provided by the heat exchanger connected to the boiler and thermal storage system.

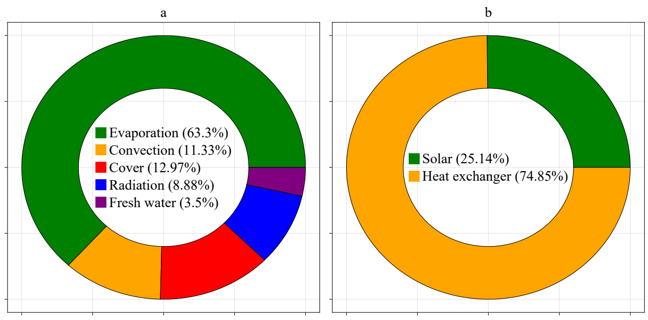

Figure 11. Distribution of the thermal power losses and heating. (a) Depicts the losses distribution with evaporation, convection, thermal cover, radiation and the fresh water added to the swimming pool. (b) Depicts the heating distribution with solar gain and heat added by the heat exchanger.

Table 3 summarizes the annual energy balance. The total heating demand of the pool reaches 1.8×10^{13} J, of which 1.67×10^{13} J is supplied by the boiler, and 0.13×10^{13} J (7.2%) by the solar thermal collectors.

5 Conclusion

This paper has presented a comprehensive dynamic

Table 3. Annual heat demand and production of the energy system.

Pool demand	*Boiler production*	*STC production*
$1.8 \times 10^{13}\ J$	$1.67 \times 10^{13}\ J$	$0.13 \times 10^{13}\ J$

simulation model of a public outdoor swimming pool, integrated with a multi-source energy system comprising a boiler, thermal energy storage (TES), and solar thermal collectors (STC). The model, implemented in Modelica, is based on fine-scale physical representations of the pool's thermal behavior, and has been used to simulate one full year of operation. It accounts for all major heat transfer phenomena, including evaporation, convection, radiation, and interactions with thermal covers. The simulation results demonstrate the model's ability to capture the nonlinear dynamics of the system and provide detailed insights into energy consumption and heat loss distributions. In particular, evaporation is identified as the dominant source of thermal losses, while the solar contribution remains modest in the current configuration.

Future work will focus on coupling this physical model with an Economic Model Predictive Control (EMPC) strategy (Blaud et al. 2023). This advanced control approach will enable the optimization of energy usage and cost by dynamically coordinating the different heat sources. The ultimate objective is to reduce operational expenditures while ensuring thermal comfort and efficient energy use.

Acknowledgements

This work was supported by Akkodis Research, France. The authors' contributions are as follows: Pierre Clément Blaud: conceptualization, methodology, software, simulation, visualization, and writing of the original draft. Imad Mourtaji: supervision and funding acquisition. The authors wish to thank Ludivine Armstrong and Daniel Longworth for their support in defining the pool parameters, and Mounina Tounkara for her valuable help in revising the language and structure of this article.

References

Bernhard, Maïté et al. (2019). "Sensitivity analysis of an outdoor swimming pool under dynamic conditions". In: *Procedia Manufacturing* 35. The 2nd International Conference on Sustainable Materials Processing and Manufacturing, SMPM 2019, 8-10 March 2019, Sun City, South Africa, pp. 124–129. DOI: 10.1016/j.promfg.2019.05.014.

Blaud, Pierre Clément et al. (2023). "From multi-physics models to neural network for predictive control synthesis". In: *Optimal Control Applications and Methods* 44.3, pp. 1394–1411. DOI: 10.1002/oca.2845.

Buscemi, Alessandro et al. (2024). "A novel model to assess the energy demand of outdoor swimming pools". In: *Energy Conversion and Management* 302, p. 118152. DOI: 10.1016/j.enconman.2024.118152.

Cour des comptes (2018). *Piscines et centres aquatiques publics: un modèle obsolète*. Tech. rep. Cour des comptes.

Delgado Marín, J.P., F. Vera García, and J.R. García Cascales (2019). "Use of a predictive control to improve the energy efficiency in indoor swimming pools using solar thermal energy". In: *Solar Energy* 179, pp. 380–390. DOI: 10.1016/j.solener.2019.01.004.

Fritzson, Peter (2011). "Modelica — A cyber-physical modeling language and the OpenModelica environment". In: *2011 7th International Wireless Communications and Mobile Computing Conference*, pp. 1648–1653. DOI: 10.1109/IWCMC.2011.5982782.

Gauthier-Clerc, François et al. (2023). "Operating data of a specific Aquatic Center as a Benchmark for dynamic model learning: search for a valid prediction model over an 8-hour horizon". In: *2023 European Control Conference (ECC)*, pp. 1–8. DOI: 10.23919/ECC57647.2023.10178287.

Kühn, Larissa et al. (2022-09). "Indoor swimming pools: a dynamic simulation model for energy analyses". In: *Proceedings of BauSim Conference 2022: 9th Conference of IBPSA-Germany and Austria*. Vol. 9. BauSim Conference. Weimar, Germany: IBPSA-Germany and Austria. DOI: 10.26868/29761662.2022.47.

Li, Yantong et al. (2021). "Swimming pool heating technology: A state-of-the-art review". In: *Building simulation*. Vol. 14, pp. 421–440. DOI: 10.1007/s12273-020-0669-3.

Liu, Jie, Sung-Chul Kim, and Ki-Yeol Shin (2021). "Feasibility Study and Economic Analysis of a Fuel-Cell-Based CHP System for a Comprehensive Sports Center with an Indoor Swimming Pool". In: *Energies* 14.20. DOI: 10.3390/en14206625.

Maier, Laura et al. (2024). "AixLib: an open-source Modelica library for compound building energy systems from component to district level with automated quality management". In: *Journal of Building Performance Simulation* 17.2, pp. 196–219. DOI: 10.1080/19401493.2023.2250521.

Petzold, Linda R (1982). *Description of DASSL: a differential/algebraic system solver*. Tech. rep. Sandia National Labs., Livermore, CA (USA).

Repository of Building Simulation Climate Data (2025). https://climate.onebuilding.org/. Accessed: 2025-02-15.

Starke, Allan R et al. (2017). "Thermal analysis of solar-assisted heat pumps for swimming pool heating". In: *Journal of the Brazilian Society of Mechanical Sciences and Engineering* 39.6, pp. 2289–2306. DOI: 10.1007/s40430-016-0671-y.

Woolley, Jonathan, Curtis Harrington, and Mark Modera (2011). "Swimming pools as heat sinks for air conditioners: Model design and experimental validation for natural thermal behavior of the pool". In: *Building and Environment* 46.1, pp. 187–195. DOI: 10.1016/j.buildenv.2010.07.014.

World Aquatics (2021). *FINA Facilities Rules*. Tech. rep. World Aquatics.

World Aquatics (2024). *Swimming Pool Certification*. Tech. rep. World Aquatics.

Yuan, Xiaolei et al. (2021). "Heating energy-saving potentials in HVAC system of swimming halls: A review". In: *Building and Environment* 205, p. 108189. DOI: 10.1016/j.buildenv.2021.108189.